International Journal of Advanced Engineering Research and Science (IJAERS)
Peer-Reviewed Journal
ISSN: 2349-6495(P) | 2456-1908(O)
Vol-11, Issue-10; Oct, 2024
Journal Home Page Available: https://ijaers.com/
Article DOI: https://dx.doi.org/10.22161/ijaers.1110.7

Comparison of LSTM and Wavelet Transform-LSTM Models for Temperature Prediction in a part of Congo Basin

Djes-Fresy Bilenga Moukodouma[1,2], Christophe Denis[2,3], Donald Romarick Rotimbo Mbourou[1], Christiane Atteke Nkoulembene[4]

[1]LAboratoire de Recherche Multidisciplinaire en Environnement (LARME), Université des Sciences et Techniques de Masuku (USTM), bâtiment du département de Chimie, Mbaya, route nationale 1, BP 901 Franceville, Gabon.
[2]Unité de Modélisation Mathématique et Informatique des Systèmes Complexes (UMMISCO), Sorbonne Université, Institut de Recherche pour le Développement, 32 avenue Henri Varagnat, 93140 Bondy Cedex, France.
[3]Institut d'Histoire et de Philosophie des Sciences et des Techniques (IHPST), Panthéon Sorbonne, 13 rue du Four, 75006 Paris, France.
[4]Département de Biologie, Université des Sciences et Techniques de Masuku, Mbaya, route nationale 1, BP 901 Franceville, Gabon.
Corresponding Author: Djes-Fresy Bilenga Moukodouma (djefresyb@gmail.com)

Received: 12 Sep 2024,
Receive in revised form: 08 Oct 2024,
Accepted: 16 Oct 2024,
Available online: 30 Oct 2024

***Keywords*— Climate change, deep learning, Long Short-Term Memory model (LSTM), Wavelet Transform, temperature prediction, biodiversity, Congo Basin.**

***Abstract*—** *Currently, the Congo Basin represents the most important center in terms of biodiversity concentration, especially with the increasing deforestation observed in the Amazon. The available climate models are mostly at larger scales, and few of them focus on specific areas of the Congo Basin, such as the locality of Makokou in Gabon. A new approach is therefore needed to predict temperatures changes in this particular region. Although some work focus on temperature prediction, most do not use deep learning algorithms. This contribution aims to compare the predictions of a Long Short-Term Memory (LSTM) model with those from the combination of Wavelet Transform and LSTM (WT-LSTM). The developed LSTM model includes two LSTM layers, two Dropout layers (with a rate of 50 %) and a Dense layer to outpout the predicted value. The WT-LSTM model shows superior results compared to the LSTM model, with a root mean square error of 0.45 °C, a mean absolute error of 0.35 °C, and a Spearman correlation coefficient of 0.97 °C. These results highlight the importance of using advanced approaches to improve climate forecasts in areas crucial for biodiversity conservation. The increased accuracy of predictions could help better anticipate and mitigate the impacts of of local climate change, thereby contributing to the sustainable management of this ecologically sensitive region.*

I. INTRODUCTION

A major challenge of the 21st century, climate change poses a real threat (Belle et al. 2016) to the flora, fauna and the daily lives of the populations in the Congo Basin (CB) (Dellink et al. 2017; Adamo et al. 2018; Grooten and Almond 2018). In practice, climate variations inhibit the reproduction of certain plant species (Chakanyuka 2019; Bush et al. 2020). Animals are increasingly moving in search of water sources and food de points (Moukodouma et al. 2023). The survival of populations is threatened by frequent floods, landslides, sometimes even earthquakes (Adamo et al. 2018; Chirwa and Adeyemi 2020; Moukodouma et al. 2023). In addition to the aforementioned impacts, soil drought is becoming more prevalent in the region (Chirwa and Adeyemi 2020). With no arable land left, many inhabitants, of the Congo Basin

are gradually dying of hunger (Chirwa and Adeyemi 2020; Toto 2023).

The impact of climate change on each species (plant, animal and human) are becoming increasingly visible. Temperature variations are a key criterion of climate change. The importance of predicting temperature evolution lies in the fact that it plays a fundamental role for all living beings. For example, some forest trees require a minimum temperature to trigger their flowering (Bush 2018; Ren et al. 2021). The human body also actually needs a certain temperature to maintain proper functioning (Vecellio et al. 2022; Vanos et al. 2023). These various observations highlight the importance of focusing on temperature variations today (Lee et al. 2023).

In this context, several models based on statistical approaches and machine learning are increasingly being used to predict temperature evolution (Piccolroaz et al. 2016; Cifuentes et al. 2020). Statistical models are commonly to extract patterns from data and to predict new observations (Piccolroaz et al. 2016). In a study conducted at three points along the Ouémé River in Benin, rainfall, average temperature, and evapotranspiration forecasts were made possible using an ARIMA (AutoRegressive Integrated Moving Average) model (Nounangnonhou and Fifatin 2016). In another **st**udy, future data were predicted based on previous meteorological data from the Aceh Besar province on the island of Sumatra, using the ETS (Error, Trend, Seasonal) univariate time series forecasting model (Jofipasi et al. 2018).

In addition to purely statistical models, the improvement in the predictive performance of machine learning has led to the emergence of many other models (Guillaume 2019; Zameer et al. 2023). In this regard, in a study, The Support Vector Machine (SVM) algorithm proved to be better at predicting global land-ocean temperatures compared to the artificial neural networks used (Abubakar et al. 2016). The SVM (Support Vector Machine) algorithm was developed by the author Vapnik (Vapnik 2013) and is used for both classification problems (where the target variable is qualitative) and regression problems (where the target variable is quantitative).

In another context, Artificial Neural Networks (ANN) have been used for predicting hourly air temperature (Li et al. 2020; Haque et al. 2021; Gong et al. 2022). These studies show that, at the regional scale, deep learning models provide much more accurate forecasts than traditional machine learning models (Abubakar et al. 2016).

All these methods provide fairly acceptable results, but they have a major drawback. Statistical models, for example, calculate the probability of a meteorological phenomenon occurring (Moazenzadeh et al. 2022). However, the mechanisms and factors affecting air temperature changes are highly complex and nonlinear, which increases the difficulty in capturing the dynamic temperature changes when predicting long time series (Hou et al. 2022). Artificial Neural Networks are a powerful tool, but they do not always manage to retain the dynamics when the time series is very large (Bharadiya 2023).

Given the major drawback that characterizes each of the previously described methods, it appears useful to migrate towards the approach of recurrent neural networks with Long Short-Term Memory (LSTM). This approach has already demonstrated remarkable results in processing long time series (Yadav et al. 2020; Karevan and Suykens 2020; Hu et al. 2020).

The issue related to the study of temperature variations affect many countries, including those in Congo Basin (CB), of which Gabon is a part. The LSTM approach could be viable option for predicting temperature changes in this region. Indeed, LSTM has the advantage of better adapting to sequential data (Xia et al. 2020; Kang et al. 2020). In a study conducted at the meteorological station in Yinchuan (China), a model based on the bidirectional LSTM algorithm has able to predict hourly air temperature with a mean absolute error of 1,02 °C(Hou et al. 2022). Other work highlighted an LSTM model for predicting both temperature and humidity levels in buildings (Wang et al. 2021). A recent study conducted in Australia revealed an average p-value of 0,9994 for the chi-squared test, thus proving that the LSTM model designed in this case predicted future temperatures in Australia with very high accuracy for one year (Qiu 2023). In the Amazon, an LSTM network has been proposed to forecast minimum, average, and maximum temperatures until 2030 in 20 major cities traversed by the forest (Dominguez et al. 2023). In another study, also in the Amazon, a neural network architecture was developed to learn to detect deforestation end-to-end from time series(Karaman et al. 2023). Regarding our target region, climate studies based on Artificial Intelligence (AI) methods are virtually non-existent. A review reported some figures regarding AI publications in Africa. To date, out of 2468 published articles in AI in Africa, Cameroon has a representation percentage of 0.85% , followed by the Democratic Republic of The Congo (DRC) at 0.45% , and Gabon at 0.16 % (Ezugwu et al. 2023). However, in Morocco, a study based on LSTM algorithm was able to predict solar radiation (Boutahir et al. 2022). In Kenya, a country with similar characteristics very similar to those of our study region, a recurrent LSTM neural network model was able to accurately forecast monthly precipitation totals (Beunk 2021).

Unlike the Amazon, where a significant number of studies on temperatures variations prevail, the issue of temperature modeling remains very understudied in the Congo Basin region.

This work compares two models for predicting temperatures in Makokou, Gabon. The first model uses the LSTM architecture alone, while the second combines Wavelet Transform with the LSTM architecture. The objective is to demonstrate how integrating the trend obtained through Wavelet Transform improves the accuracy of temperature forecasts compared to the LSTM-only model.

This contribution is essential in a region that has long been forgotten, yet remains the largest carbon sink in the world today (Atyi et al. 2022). Governments and actors of the Conference of The Parties (COP) and the Intergovernmental Panel on Climate Change (IPCC) aim to keep the rise in global temperature within the 1.5°C threshold (MAIDOU 2020; Beaudoin and Chaloux 2023; Torre-Schaub 2023). This study could thus help the governments of the Congo Basin (CB) better plan their environmental policies to meet this objective.

Our contribution is organized as follows: Section II, Materials and Methods, presents the study area and the methodology followed. Section III, Results, highlights the main findings of the study. Section IV, Discussion, elaborates on the various results in light of the bibliographical references. Section V is the Conclusion, which allows us to summarize the study and outline future work that could further enrich the current research.

II. MATERIALS AND METHODS

1. Study area

The study takes place in the locality of Makokou, the capital of the Ogooué-Ivindo province in northeastern Gabon (Figure 1). Gabon occupies the largest portion of the Congo Basin forest (Balada 2021). This forest is predominantly found in The Ogooué-Ivindo region, particularly in the Ipassa-Makokou Biosphere Reserve and the Ivindo National Park (Roland et al. 2016). These two reserves alone host a diverse range of plant and animal species (Roland et al. 2016; Laguardia et al. 2021). Among them, there are approximately 18 species of mammals, 424 species of birds, 65 species of reptiles, and 47 species of amphibians (Roland et al. 2016). Additionnaly, the elephant, the forest's ecological engineer is present in large numbers in the Ogooué-Ivindo province (Berzaghi et al. 2019; Laguardia et al. 2021; Kermabon 2022). Like the rest of the country, the locality of Makokou has an equatorial climate characterized by alternating dry and rainy seasons (Roland et al. 2016). The average temperature in Makokou hovers around 24°C, and the annual average rainfall ranges between 1600 mm and 1800 mm (Roland et al. 2016).

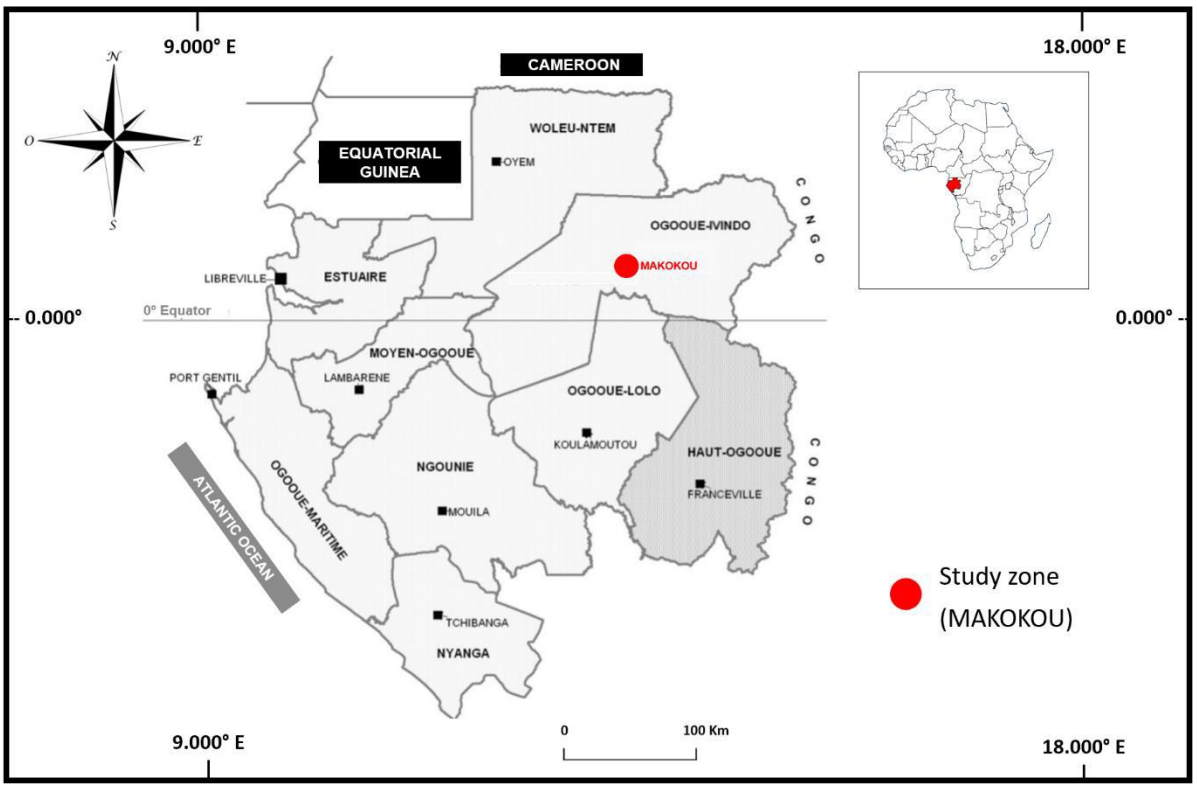

Fig.1: Location of study area

Thus, the locality of Makokou stands out as an area with a high concentration of biodiversity. This significant biodiversity warrants attention, considering the multiples roles it could play for human survival, as well as for the fauna and flora. It could also be a key driver in the fight against climate change.

2. Description of the Database

The climatic data for our study are from the locality of Makokou for the period 2000-2020. They were collected by the National Climatic Data Center (NCDC). The NCDC is a major global repository of meteorological data (Gad and Hosahalli 2022).Regarding our study area, only the period 2000 to 2020 was recorded, with a significant number of daily observations (approximately 4,695 observations were counted).

As illustrated in Tables 1a and 1b, many climatic parameters are measured at this station. The database contains the date of the day (YEARMODA), the average temperature (TEMP) in degrees Fahrenheit, the average dew point in degrees Fahrenheit (DEWP), the average sea-level pressure in millibars (SLP), the station's average pressure for the daily in millibars (STP), the visibility (distance to which objects can be clearly seen in meters) (VISIB), maximum temperature in degrees Fahrenheit (MAX), mimimum temperature in degrees Fahrenheit (MIN), total precipitation in inches (PRCP), and all weather conditions (FRSHTT). Specifically, in the acronym FRSHTT, we find Fog, Rain, Snow, Hail, Thunder, and Tornado.

Table 1a : Characteristics for the first 5 rows for the first 5 variables [source : NCDC]

YEARMODA	TEMP	DEWP	SLP	STP	VISIB
01/01/2000	70.5	69.2	1006.9	950.2	6.2
02/01/2000	74.1	68.7	1006.9	949.9	4.7
03/01/2000	74.6	70.6	1006.2	949.2	6.5
04/01/2000	74.8	70.7	1005.8	949.4	7.4
05/01/2000	74.2	70.8	1005.2	948.8	5

Table 1b : Characteristics for the first 5 rows for the other variables [source : NCDC]

YEARMODA	MAX	MIN	PRCP	FRSHTT
01/01/2000	75.2	68.4	0.39E	10
02/01/2000	84.9	65.5	0.03G	100000
03/01/2000	84.6	66.9	0.00G	100000
04/01/2000	84.6	67.1	0.00D	100000
05/01/2000	80.6	68.4	0.02E	100010

During our study, the available database was divided into two parts: one part was used for training future mordels (which accounted for 80 % of the data), and the remaining 20 % of the data was used to testing the neural network models developed in this study.

III. METHODS

3.1 Discrete Wavelet Transform (DWT)

The Discrete Wavelet Transform (DWT) is a discretized version of the Continuous Wavelet Transform (CWT), where the signal analyzed at specific scales and positions (Alessio 2016; Guo et al. 2018). Unlike the CWT, The DWT does not produce redundancy, making it more efficient for data storage and processing (Ponni alias Sathya and Ramakrishnan 2020; Chen et al. 2021).

In our study, we opted for Symlets of order 4 (Sym4). Unlike Daubechies wavelets, which have a non-symmetric support, Symlets are nearly symmetric. This symmetry makes these wavelets more suitable for certain applications, such as image processing and denoising, where edge effects are less tolerable (Shahbaztabar et al. 2018 ; Isabona and Kehinde 2019 ; Arfaoui et al. 2021). Additionally, like Daubechies, Symlets are orthogonal wavelets (Guo et al. 2022; Daud and Sudirman 2022). This property allows for decomposition and reconstruction without loss of information, which is essential for many signal processing applications (Kumar and Satyanarayana 2022). Finally, Symlets are effective for smoothing a signal, meaning they

can eliminate small irregularities while preserving larger trends (Gossler et al. 2023).

Before passing the temperature data to the LSTM neural network model, we applied a Discrete Wavelet Transform to the time series of average temperatures from the locality of Makokou. We then extracted the last component from the wavelet decomposition. This last component represents the trend, typically observed in the low frequencies. The extracted trend from the signal was saved in the database to be useful for the development of the models.

3.2 Development of Neural Networks Models

3.2.1 Long Short-Term Memory Model

Long Short-Term Memory (LSTM) is a type of recurrent neural network designed to overcome some limitations of traditional recurrent neural networks. The limitations of these traditional recurrent neural networks are related to learning long-term dependencies in data sequences. LSTM indeed has the advantage of being better suited for sequential data (Xia et al. 2020 ; Bagastio et al. 2023).

An LSTM network consists of a series of LSTM cells (or blocks). Each of these cells has a complex internal structure that allows it to retain, forget, or modify information based on the input data sequence (Qiu 2023).

The following Figure 2 presents the general architecture of an LSTM network.

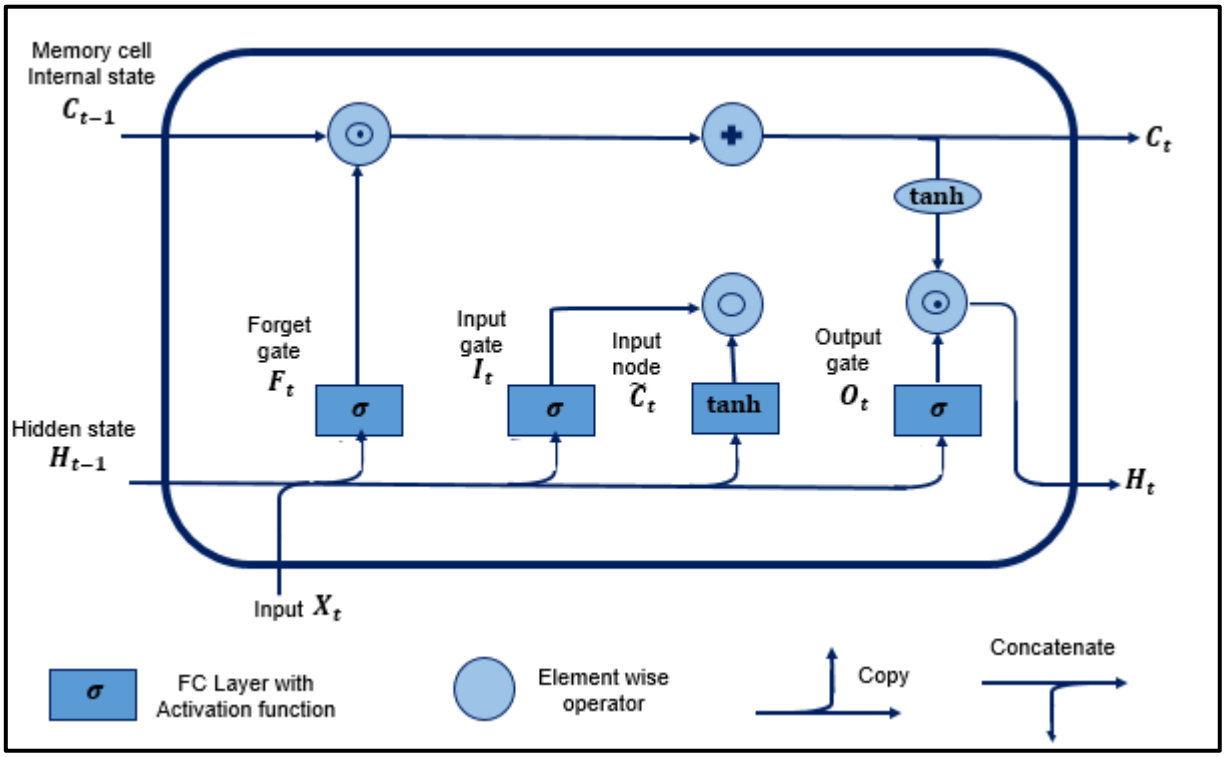

Fig.2: Architecture of LSTM Network [source: internet]

In the context of our study, we developed a five-layer LSTM model. This model consisted of two LSTM layers, two Dropout layers, and one Dense layer. In practice, the two LSTM layers (each with 50 units) function as memory blocks than can retain long-term information. To prevent overfitting, we added two Dropout layers with a rate of 50 %, meaning that 50 % of the neurons were randomly disabled during each iteration in the developed LSTM model. This regularization technique aimed to prevent the network from becoming too dependent on specific neurons during training.

Once the model was constructed, it was compiled using the Adam optimizer and the ‘’Mean_Squared_Error” loss function. Compilation is necessary as it configures the model for learning while clearly specifying how it should be trained.

Immediately after compiling the model, we trained it using the training dataset (80 % of the data). We then used our model to make predictions on the test data. Afterward, we reversed normalization process to bring the predicted values back to their original scale. Finally, we visually compared these predictions with the actual values to evaluate their correspondence.

The last step of our modeling involves interpretability. At this stage, we aim to assess the contribution of each explanatory variable to the model. To achieve this, we used Shapley values, which provide a consistent and fair method

for quantifying the impact of each explanatory variable on the model's prediction (Denis and Varenne 2022).

3.2.2 Performance Evaluation Criteria for the Models

3.2.2.1 Traditional Metrics

The models were primarily evaluated using three traditional metrics : Root Mean Square Error (RMSE), Mean Absolute Error (MAE), and Mean Absolute Percentage Error (MAPE) (Boutahir et al. 2022; Ezugwu et al. 2023).

The RMSE is defined by the following equation (1):

$$RMSE = \sqrt{\frac{1}{N}\sum_{i=1}^{N}(Y_i - y_i)^2} \qquad (1)$$

In this formula, N represents the number, of observations, Y_i is the actual value, and y_i is the predicted value.

The Mean Absolute Error (MAE) defined by equation (2), is the average of the absolute differences between the prediction y_i and the actual value Y_i over a sample of N observations.

$$MAE = \frac{1}{N}\sum_{i=1}^{N}(|Y_i - y_i|) \qquad (2)$$

Starting from equation (2), we can assert that the smaller the MAE, the better the model in relation to the data.

The Mean Absolute Percentage Error (MAPE) is a statistical indicator used to measure the accuracy of a forecasting model. It represents the average error between actual values and predicted values, expressed as a percentage. More specifically, MAPE calculates the average of the absolute percentage errors of the actual values, allowing us to understand how closely or distantly a model's predictions align with the observed values. The formula for MAPE is as follows :

$$MAPE = \frac{1}{N}\sum_{i=1}^{N}\left|\frac{Y_i - y_i}{y_i}\right| \times 100 \qquad (3)$$

Where N represents the number of observations, Y_i is the actual value, and y_i is the predicted value.

If the MAPE is low, it indicates that the model is accurate (the predictions are close to the actual values). Conversely, if the MAPE is high, it suggests that there is a significant discrepancy between the model's predictions and the actual values.

3.2.2.2 Wilcoxon Signed-Rank Test

The Wilcoxon Signed-Rank Test is used to compare paired samples, such as the actual values and the predictions of a model. The null hypothesis of this test states that the medians of the differences between the pairs are equal to zero. The alternative hypothesis states that the medians of the differences between the pairs are not equal to zero.

The Wilcoxon Signed-rank Test first calculates the differences for each pair of paired values. It then assigns absolute ranks to the differences by ordering them from smallest to largest. After that, the ranks of the differences are reassigned based on their original signs. Next, the test calculates the sum of the ranks for the positive differences and for the negative differences. Finally, the signed rank sums are used to compute the test statistic, which is compared to a reference distribution to determine significance.

Regarding interpretation, if the test statistic is large or small and the p-value is above the significance threshold (0.05), we do not reject the null hypothesis. However, if the previous conditions are not met, the null hypothesis is rejected.

3.2.2.3 Spearman's Rank Correlation Coefficient

Spearman's Rank Correlation Coefficient is a statistical measure that evaluates the strength and direction of a monotonic relationship between two variables (Astivia and Zumbo 2017). It is based on three key principles : monotonic relationship, ranks, and its formula (Al-Hameed and Khawla 2022).

A relationship is considered monotonic if, as the values of one variable increase, the values of the other variable consistently either increase or decrease, though not necessarily in a linear manner.

Instead of directly comparing the raw values of the variables, Spearman relies on ranks. The values of the variables are first ranked, and then the differences between these ranks are used to calculate the correlation. Since it is based on ranks rather than raw values, Spearman's method is less sensitive to outliers.

The Spearman rank correlation coefficient (ρ) is calculated from the difference in ranks between the two variables, following the formula provided in equation (5) (Eltehiwy and Abdul-Motaal 2023)

$$\rho = 1 - \frac{6\sum {d_i}^2}{n(n^2 - 1)} \qquad (5)$$

Where d_i is the difference between the ranks of each pair of variables and n being the number of data pairs.

If $\rho = 1$, the relationship is perfectly monotonic and increasing, and if $\rho = -1$, the relationship is perfectly monotonic and decreasing. In the case where ρ is zero, there is no monotonic relationship between the variables.

3.2.2.4 Test de Mann-Whitney U

To further strengthen the model results, we used the Mann-Whitney U Test to compare the median residuals of different models to see if there is a significant difference between their distributions (Vengatesan et al. 2018; Vierra et al. 2023).

The null hypothesis (H_0) of this test states that there is no significant difference between the two samples. In other words, the samples have similar distributions. Conversely, the alternative hypothesis (H_1) states that there is a significant difference between the distributions, meaning that one of the models tends to produce larger or smaller values than the other.

The Mann-Whitney U Test begins with ranking the data. The data from both samples are first combined and ordered from smallest to largest. Then, ranks are assigned to the values. If two or more values are identical, they receive the average of the ranks they would occupy if they were distinct.

After determining the ranks of the data, the calculation of the U statistics follows. For each sample, The Mann-Whitney U Test calculates a U score based on the sum of the ranks. The basic formulas are given in equations (3) et (4) (Wall Emerson 2023)

$$U_1 = R_1 - \frac{n_1(n_1+1)}{2} \quad (3)$$

$$U_2 = R_2 - \frac{n_2(n_2+1)}{2} \quad (4)$$

Where R_1 and R_2 representing the sums of ranks for samples 1 and 2, respectively, and n_1 and n_2 representing the sizes of samples 1 and 2.

The third step of the test is the selection of the U statistic. In practice, the smaller of the two U values is used to interpret the test.

Finally, the associated p-value is calculated from the U statistic to determine if the observed difference between the samples is significant. If the p-value is less than a threshold (often set at 0.05), we reject the null hypothesis in favor of the alternative hypothesis.

IV. RESULTS

1. Data exploration

The exploration of the database reveals that the daily average temperatures in the locality of Makokou fluctuate between 20 °C and 32 °C during the study period (2000-2020) (Figure 3).

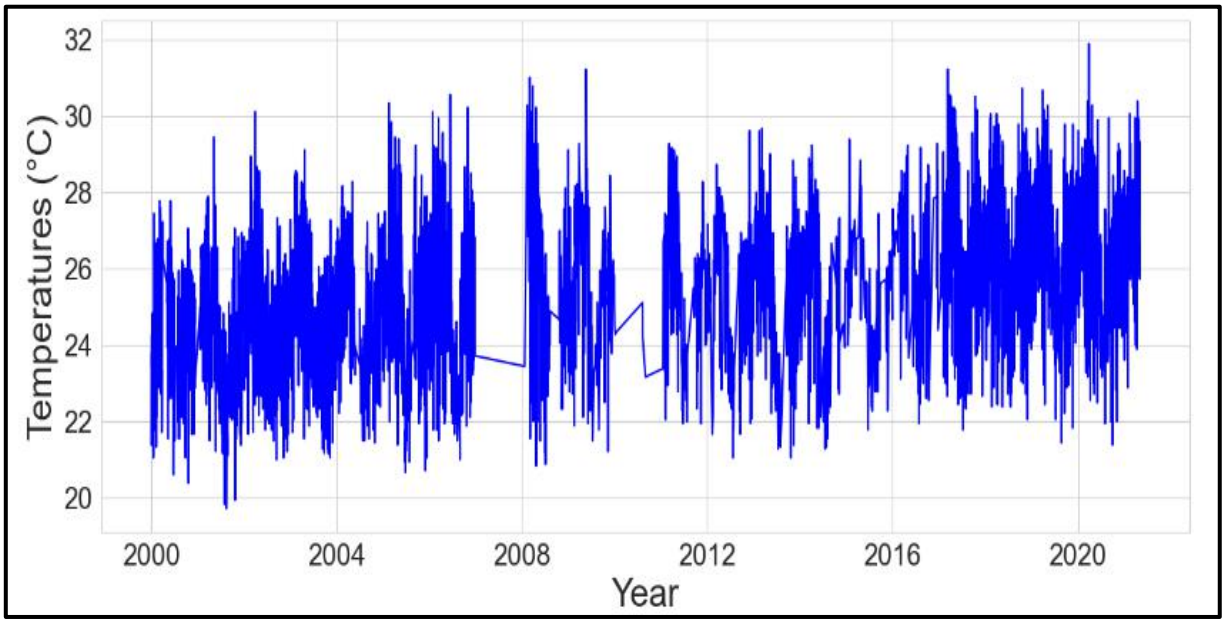

Fig.3: Evolution of Temperature Time Serie

As illustrated in Figure 3, the trend extracted after applying the Discrete Wavelet Transform shows a similar evolution to the raw data.

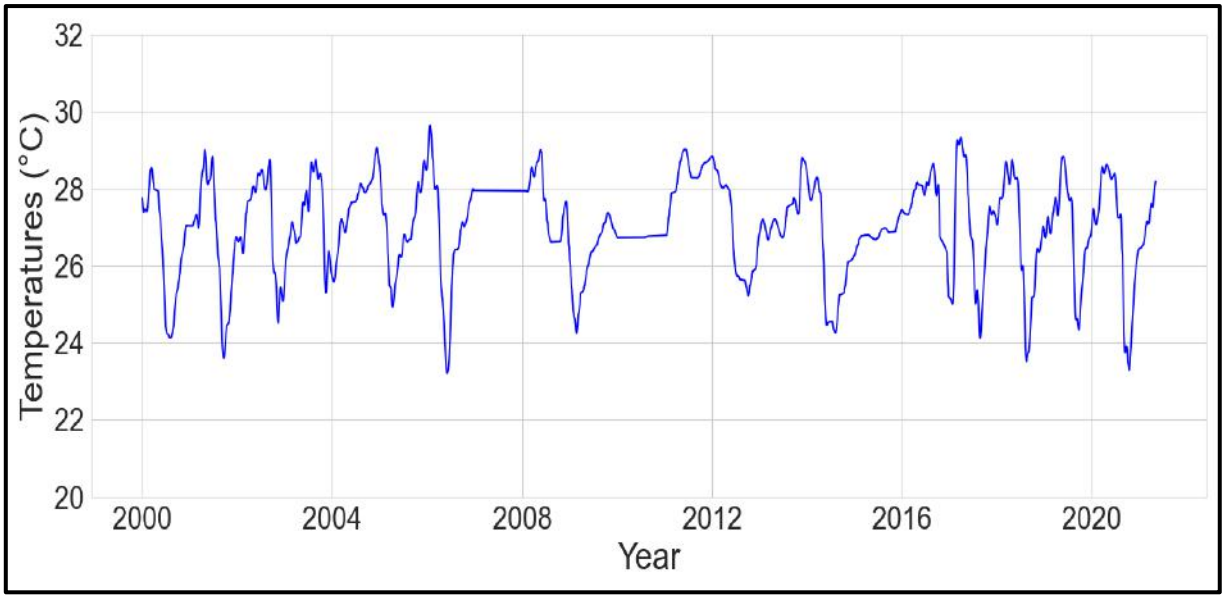

Fig.4: Temperature Trends

The similarity with the raw data suggests that the trend is relevant for modeling temperatures in the locality of Makokou.

2. Neural Network Models and Results

2.1 Long Short-Term Memory Model (LSTM) and Performance Evaluation.

Once the LSTM model was designed, we trained it (figure 5) and then tested it with the test data (figure 6). The following Figure 5 shows how the training and validation losses evolve during the model's learning phase.

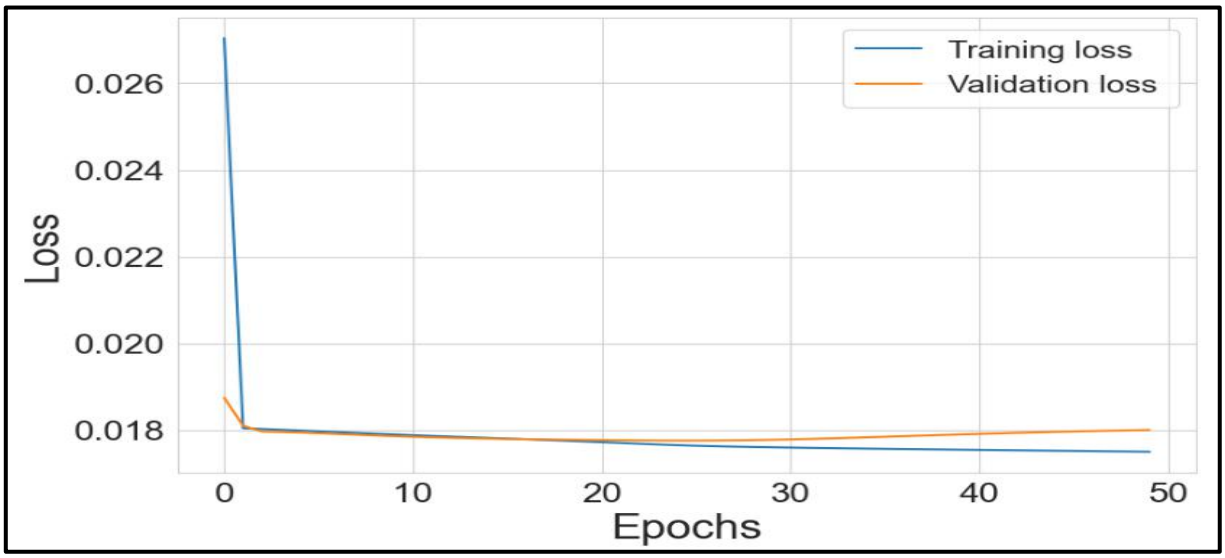

Fig.5: Training and validation loss curves of the LSTM model

Predictions were then made after training the model. Figure 6 highlights the results obtained.

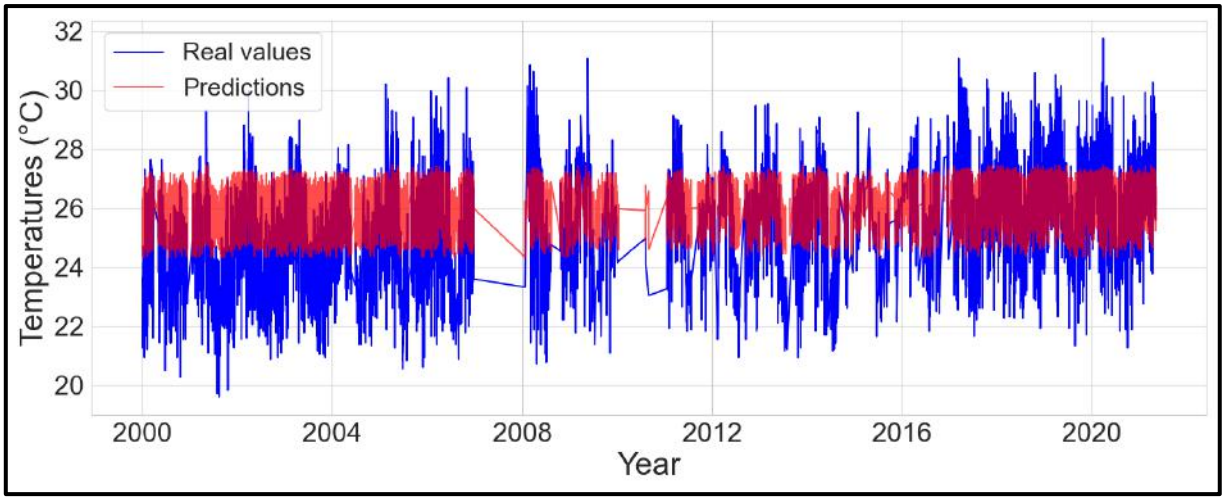

Fig.6: Actual values and LSTM Model Predictions

The observation of Figure 6 reveals that the simple LSTM model, which had not undergone any prior transformation, does not predict temperatures satisfactorily. The traditional evaluation metrics yielded a value of 1.62 °C for the root mean square error, 1.30 °C for the mean absolute error, and a mean absolute percentage error of 4.89 %.

To further evaluate the simple LSTM model, we conducted non-parametric Wilcoxon signed-rank test and the Spearman correlation coefficient. The Wilcoxon signed-rank test indicates a significant difference between the actual values and the predicted values (Table 2)

Table 2: Wilcoxon signed-rank test Results

	Wilcoxon signed-rank	
	Statistic of Test Z	**p-value**
LSTM	137748	1.12×10^{-21}

The Spearman correlation coefficient (Table 3) suggests a moderate significant correlation between the original values and the model's predictions.

Table 3: Spearman Correlation Coefficient Test Results

	Spearman's rank correlation	
	Correlation coefficient ρ	**p-value**
LSTM	0.40	8.25×10^{-34}

The hyperparameters of the developed LSTM neural network are listed in Table 4. These hyperparameters are parameters that we intuitively selected before training the model, with the aim of minimizing the evaluation metrics.

Table 4: LSTM Model hyperparameters

Parameters	**Values**
Number of Units LSTM	50
Epochs	50
Batch_size	32
Optimizer	Adam
Learning rate	0.001
Dropout rate	0.5

2.2 Wavelet Transform (WT) combined with Long Short-Term Memory Model (LSTM))

In order to improve the performance our previously designed LSTM Model, we replaced the raw data (average temperatures) with the trend extracted from the Wavelet Transform. Then, the model was trained for 50 epochs. Figure 7 illustrates the evolution of the training and validation losses.

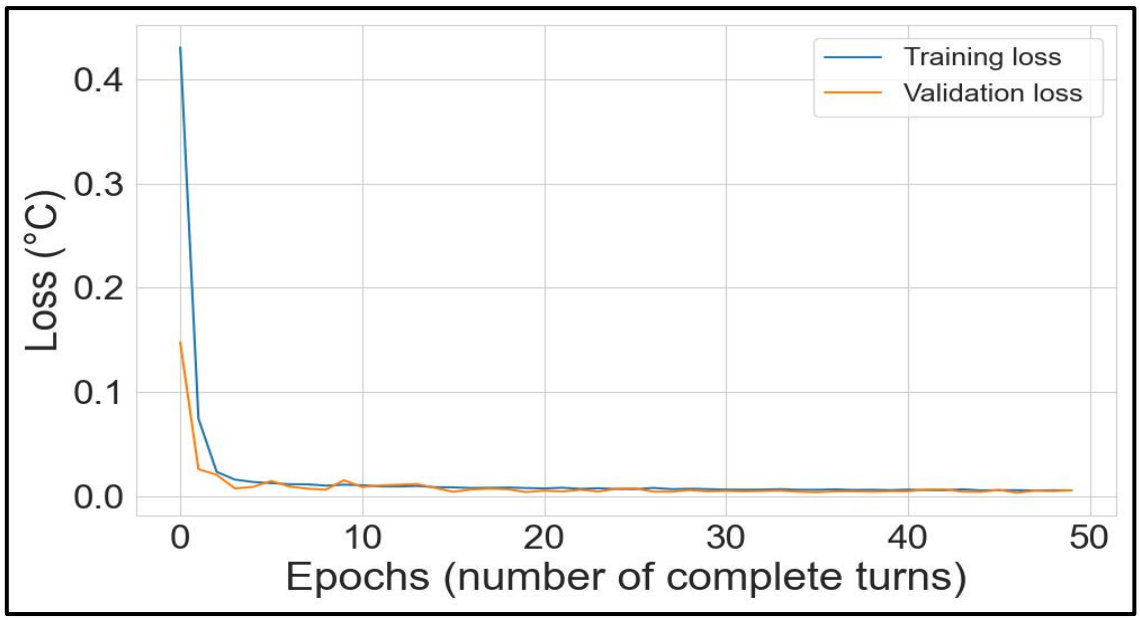

Fig.7: Evolution of the training and validation loss curves during the training process

There appears to be an overlap of the training and validation loss curves during the training process (Figure 7). Figure 8 highlights the predictions obtained from this new LSTM model. We observe that this time, there is an almost perfect match between the original data and the predictions.

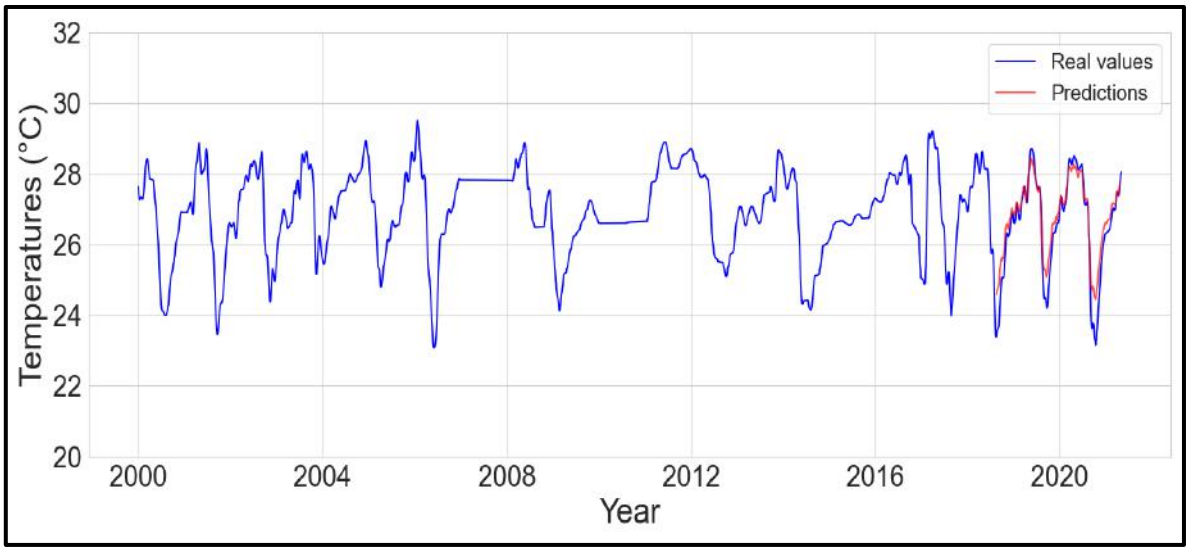

Fig.8: Actual values and Predictions of the WT-LSTM Model

The Root Mean Squared Error (RMSE), Mean Absolute Error (MAE) and Mean Absolute Percentage Error (MAPE) are 0.45 °C, 0.35 °C and 1.35 %, respectively.

The Wilcoxon Signed-Rank Test indicates that there is no significant difference between the real values and the predicted values (Table 5), which seems to confirm that the predicted values closely match the original values.

Table 5: Wilcoxon signed-rank Test Results

	Wilcoxon signed-rank	
	Statistic of Test *Z*	**P-value**
WT-LSTM	126748	0.08

The Spearman Correlation Coefficient (Table 6) suggests a strong and significant correlation between the original values and the model's predictions.

Table 6: Spearman Correlation Coefficient Test Results

	Spearman's rank correlation	
	Correlation coefficient ρ	**P-value**
WT-LSTM	0.97	0

The Mann-Whitney U Test reveals a significant difference between the residuals of the simple LSTM model and the WT-LSTM (Table 7)

Table 7: Mann-Whitney U Test Results

	Mann-Whitney U Test	
	Statistic U	**p-value**
WT-LSTM	3255419	9.71×10^{-75}

Finally, we evaluated the contributions of each explanatory variable to the output of the WT-LSTM model using Shapley indices (Figure 9). This calculation shows that the average dew point (DEWP), the mean sea level pressure (SLP), and the mean station pressure for the day (STP) strongly influence the model's output

This suggests that these variables play a crucial role in the predictions. Following these top three variables, other variables include visibility (VISIB), maximum temperatures (MAX), and minimum temperatures (MIN), which have nearly equal contributions (0.018). Lastly, we find total precipitation (PRCP) and the variable FRSHTT, which summarizes weather conditions.

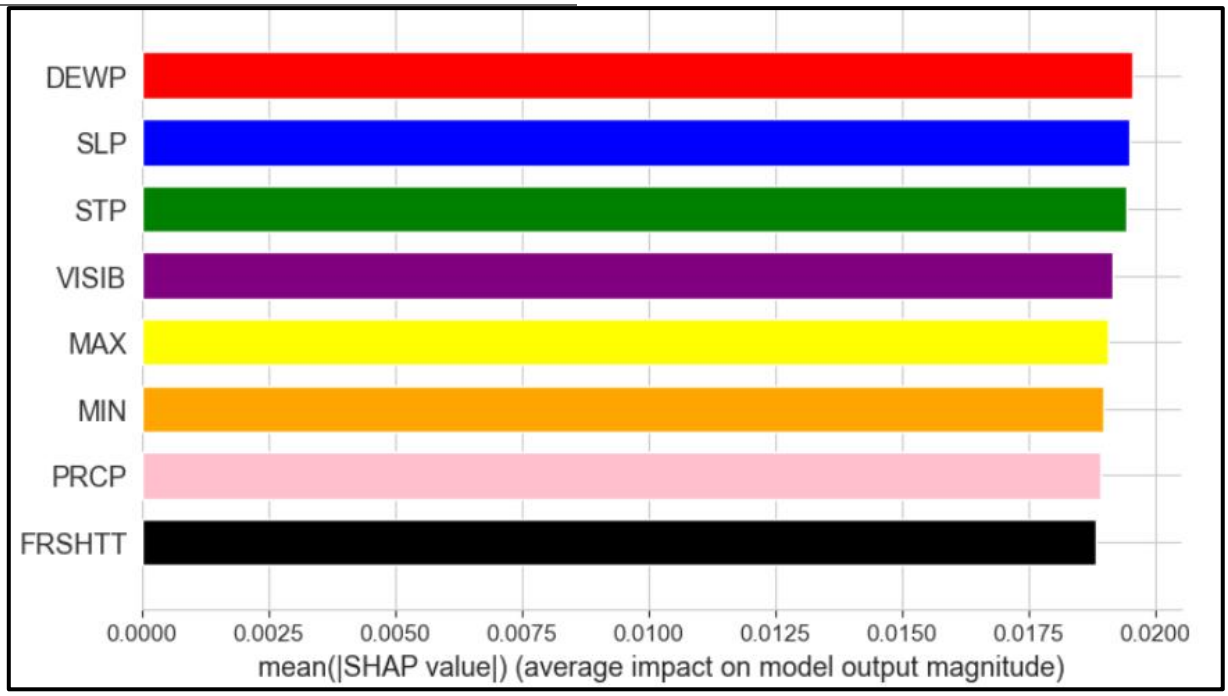

Fig.9: Contributions of explanatory variables to the WT-LSTM Model

V. DISCUSSION

For the 10th epoch during the training phase of our simple LSTM model, model convergence seems to appear. However, for the WT-LSTM model, convergence is observed earlier (around the third epoch) and is noticeable throughout the training, with training and validation losses oscillating around zero. This very rapid convergence of the WT-LSTM model could be explained by the presence of training data that is quite representative of the overall dataset and effective hyperparameter choices for the models. Indeed, the evaluation metrics RMSE, MAE and MAPE are respectively 0.45 °C, 0.35 °C et 1.35 %. Such values for our performance indicators suggest that the gap between predictions and actual values is minimal. These results seem to align with those obtained in a study by Park et al (Park et al. 2019). In this study, an LSTM model was also designed to predict temperature over short periods (6, 12 and 24 hours) and then extended to 7 and 14 days. This LSTM model consisted of 4 LSTM layers and 384 neurons (or units). The RMSE obtained in that study was 0.79 °C for the 24-hour prediction, 2.84 °C for the 7-day prediction, and 3.06 °C for the 14-day prediction. Furthermore, our results appear to be consistent with those obtained in another study (Inik et al. 2022). This study analyzed a ground temperature dataset from 2013 to 2021 in Turkey using an LSTM model to predict the average temperature. In this analysis, the authors developed a hybrid LSTM-GRU model able of predicting the average ground temperature in

Bingöl (Turkey). The developed model had hyperparameters of a learning rate of 0.001, two layers (LSTM et GRU), each with 200 units, and a Dense layer for the final model ouput. The RMSE achieved was $1.25\ °C$. All the metric values obtained in these various studies are close to ours. Although not working on the same dataset in each case, this comparison with these different studies is still useful, as it addresses the same problem and utilizes the same LSTM strategy. We demonstrate in our work that with a low number of layers (2 LSTM layers) and neurons (50), our simple LSTM model yields less satisfactory predictions. However, after extracting the trend via a Wavelet Transform, The WT-LSTM model maintaining the same number of LSTM layers and units now predicts temperatures better, with minimal discrepancies between actual values and predicted values.

The Wilcoxon signed-rank test reveals a significant difference between the actual and predicted values for the simple LSTM model, with a p-value of 1.12×10^{-21}. In contrast, for the WT-LSTM model, the Wilcoxon signed-rank test suggests that there is no significant difference between the actual and predicted values. These results indicate that while the simple LSTM model may be effective in certain situations, it fails to capture specific fluctuations in the temperature time series in this case. On the other hand, the p-value (0.08) exceeding the significance threshold (0.05) in the latter case emphasizes that the combination of Wavelet Transform and LSTM is well suited to better capture the underlying complex relationships in temperature data. Integrating the Wavelet Transform into the LSTM structure significantly enhances its ability to capture multi-scale variations and fluctuations in time series.

Several studies confirm the effectiveness of integrating the Wavelet Transform into predictive models. In this regard, a recent study explores the combined use of Wavelet Transform and LSTM for weather data forecasting, showing that this combination allows for a significant improvement in prediction accuracy, particularly for non-stationary time series. The study demonstrated that the prediction of the distillation column temperature was improved by 10 % using the LSTM network when the data were pre-transformed via the Wavelet Transform (Kwon et al. 2022). Another article indicates that neural network models based on the Wavelet Transform achieved better performance in predicting climatic time series with improved capture of variations at different scales. This study specifically employed the combination of Wavelet Transform and LSTM to predict daily average temperature in the city of Mugla (Turkey). The study noted that with this combination, the model outperformed the standard LSTM, achieving a mean squared error of $0.56\ °C$ (Ghasemlounia et al. 2024).

The Spearman correlation coefficient is 0.40 for the LSTM model. Although this value is statistically significant with a p-value of 8.25×10^{-34}, which is less than 0.05, it indicates a moderate correlation coefficient between the predicted and actual values. This moderate correlation suggests that the simple LSTM model does not sufficiently capture the complex relationships present in the data. However, for the WT-LSTM model, the Spearman correlation coefficient reaches an impressive value of 0.97 with a p-value of zero, indicating an almost perfect correlation between the predicted and actual values. This confirms that the WT-LSTM model is effective in capturing and reproducing the trends in real data, thus providing accurate and reliable predictions.

In a complementary study (Vikas Goyal et al. 2022), the authors demonstrated that the Spearman correlation coefficient is a relevant performance criterion for evaluating temperature forecasting models, such as those using LSTM neural networks. They observed that the Spearman correlation coefficient was statistically significant across all evaluated models, reinforcing its usefulness in validating model performance.

Additionally, The Mann-Whitney U Test reveals a significant difference between the residuals of the simple LSTM and WT-LSTM models. This difference indicates that the two models are not equivalent in their ability to predict average temperature in the locality of Makokou. The results of the Mann-Whitney U Test, combined with the Spearman correlation coefficient, suggest that the WT-LSTM model may offer superior performance compared to the simple LSTM model. This tests thus support the notion that the WT-LSTM is not only more accurate in terms of prediction precision but also more robust in capturing the complexities of the data. In another study, models were developed to predict temperature in wind farms (Mishra et al. 2020). The comparison of these models showed that those based on Wavelet or Fourier Transforms exhibit better performance, demonstrating the added value these transforms bring to deep learning model predictions.

Shapley values reveal that the average dew point (DEWP), mean sea level pressure (SLP), and average station pressure for the day (STP) significantly influence the model's output. Indeed, the average dew point is an important indicator for predicting fog, rain, or snow formation, which directly influences temperature predictions via weather models. A study analyzed the relationships between air temperature and the average dew point in the United States (Russell 2024).The study demonstrates that the average dew point plays a key role in predicting temperatures and

precipitation, as it is closely related to air humidity. Specifically, the higher the average dew point, the more moisture the air contains, which directly affects the weather models used to predict temperatures. The authors conclude that considering the average dew point in prediction models improve forecast accuracy, particularly for extreme weather events such as heatwaves or heavy rainfall.

Moreover, mean sea level pressure and station pressure significantly influence large-scale weather phenomena such as temperatures. Indeed, atmospheric pressure affects temperature by influencing air density and its ability to retain heat. For instance, in a high-pressure area, air descends, which may lead to an increase in temperatures due to adiabatic compression. Conversely, in a low-pressure area, air rises, which can lead to a decrease in temperatures (Ning et al. 2018). In this regard, a study showed that deep learning predictive models (like LSTMs) typically exploit sea level pressure to forecast events such as storms, confirming the considerable contribution of sea level pressure in predicting climatic variables (Rus et al. 2023).

Although it has the lowest Shapley contribution, the variable FRSHTT, which summarizes the weather conditions of Fog, Rain, Snow, Hail, Thunder and Tornado, also influences the model's output. This rightly confirms the predominant role of weather conditions in temperature prediction. This is supported by recent studies (Cifuentes et al. 2020; Azari et al. 2022) that present a significant number of studies showing that various weather conditions, including total precipitation and maximum temperature, greatly influence global, regional, or even local temperatures predictions.

VI. CONCLUSION

The major objective of our study was to predict temperature in the locality of Makokou by utilizing a database of climate parameters covering the period from 2000 to 2020. In this context, two deep learning models were proposed: the first based on a classic LSTM architecture, and the second incorporating a Wavelet Transform (WT-LSTM) to capture underlying trends and variations in the time series.

Model validation relied on traditional metrics such as the Root Mean Square Error (RMSE), Mean Absolute Error (MAE), and Mean Absolute Percentage Error (MAPE). Additionally, non-parametric tests, namely The Wilcoxon signed-rank test, The Spearman correlation coefficient, and the Mann-Whitney U test, were employed to reinforce the validation criteria for the models.

The results obtained showed an RMSE of 0.45°C for the WT-LSTMTO, compared to 1.62°C for the simple or standard LSTM model. These results indicate that the model based on the Wavelet Transform (WT-LSTM) effectively captures complex relationships in the meteorological data. The Wilcoxon signed-rank test revealed no significant differences between the predictions of the WT-LSTM model and the actual values. This conclusion is reinforced by the Spearman correlation coefficient, which reached a value of 0.97 for the WT-LSTM model. This value, significant correlation between the predictions of the WT-LSTM model and the actual values.

Moreover, the Mann-Whitney U test highlighted a significant difference between the residuals of the two models, demonstrating that the two architectures do not capture the underlying relationships in the data identically. This confirms that the WT-LSTM model, which incorporates the Wavelet Transform, is better suited to model complex climatic trends in temperature time series.

In conclusion, this study demonstrates that adding the Wavelet Transform to an LSTM architecture significantly enhances the predictive performance of recurrent neural networks, particularly in the context of long-term temperature forecasting. It would be interesting in future studies to explore the integration of this model with other advanced deep learning techniques and to apply this method to order climate parameters such as rainfall, in order to generalize these results and improve the understanding of meteorological dynamic in various regions of the Congo Basin.

CODE AVAILABILITY

The Python codes for all scripts used in this study are available upon request from the corresponding author.

ACKNOWLEDGMENT

We would like to thank the Institute for Research and Development (IRD) for its multifaceted support throughout these years of doctoral study.

CONFLICTS OF INTEREST

The authors declare that they have no conflicts of interest

REFERENCES

[1] Abubakar A, Chiroma H, Zeki A, Uddin M (2016) Utilising key climate element variability for the prediction of future climate change using a support vector machine model. International Journal of Global Warming 9:129–151. https://doi.org/10.1504/IJGW.2016.074952

[2] Adamo N, Al-Ansari N, Sissakian VK, et al (2018) Climate Change : Consequences on Iraq's Environment. Journal of Earth Sciences and Geotechnical Engineering 8:43–58
[3] Alessio SM (2016) Discrete Wavelet Transform (DWT). In: Alessio SM (ed) Digital Signal Processing and Spectral Analysis for Scientists: Concepts and Applications. Springer International Publishing, Cham, pp 645–714
[4] Al-Hameed AA, Khawla (2022) Spearman's correlation coefficient in statistical analysis. International Journal of Nonlinear Analysis and Applications 13:3249–3255. https://doi.org/10.22075/ijnaa.2022.6079
[5] Arfaoui S, Mabrouk AB, Cattani C (2021) Wavelet Analysis: Basic Concepts and Applications. Chapman and Hall/CRC, New York
[6] Astivia OLO, Zumbo BD (2017) Population models and simulation methods: The case of the Spearman rank correlation. British Journal of Mathematical and Statistical Psychology 70:347–367. https://doi.org/10.1111/bmsp.12085
[7] Atyi R, Hiol H, Lescuyer G, et al (2022) Les Forêts du bassin du Congo : Etat des Forêts 2021. In: Centre de Recherche Forestière Internationale (CIFOR)
[8] Azari B, Hassan K, Pierce J, Ebrahimi S (2022) Evaluation of Machine Learning Methods Application in Temperature Prediction. CRPASE 8:1–12. https://doi.org/10.52547/crpase.8.1.2747
[9] Bagastio K, Oetama RS, Ramadhan A (2023) Development of stock price prediction system using Flask framework and LSTM algorithm. Journal of Infrastructure, Policy and Development 7:. https://doi.org/10.24294/jipd.v7i3.2631
[10] Balada A (2021) Le Bassin du Congo, deuxième puits de carbone du monde entre préservation et exploitation. Le Monde.fr
[11] Beaudoin S, Chaloux A (2023) Négociations climatiques : COP 27 à la COP 28, Observatoire Multilatéralisme & Organisations internationales. https://observatoire-multilateralisme.fr/publications/negociations-climatiques-cop-27-a-la-cop-28/. Accessed 10 Jan 2024
[12] Belle EMS, Burgess ND, Misrachi M (2016) Impacts du changement climatique sur la biodiversité et les aires protégées en Afrique de l'Ouest, Résumé des résultats du projet PARCC, Aires protégées résilientes au changement climatique en Afrique de l'Ouest. Rapport UNEP-WCMC 52p
[13] Berzaghi F, Longo M, Ciais P, et al (2019) Carbon stocks in central African forests enhanced by elephant disturbance. Nat Geosci 12:725–729. https://doi.org/10.1038/s41561-019-0395-6
[14] Beunk J (2021) Seasonal Forecasting of Rainfall in Equatorial East Africa using an Artificial Neural Network. Master Thesis
[15] Bharadiya J (2023) Exploring the Use of Recurrent Neural Networks for Time Series Forecasting. International Journal of Innovative Research in Science Engineering and Technology 8:2023. https://doi.org/10.5281/zenodo.8002429
[16] Boutahir MK, Farhaoui Y, Azrour M (2022) Machine Learning and Deep Learning Applications for Solar Radiation Predictions Review: Morocco as a Case of Study. In: Yaseen SG (ed) Digital Economy, Business Analytics, and Big Data Analytics Applications. Springer International Publishing, Cham, pp 55–67
[17] Bush ER (2018) Tropical Phenology In A Time Of Change. https://doi.org/Phd Thesis, Stirling University
[18] Bush ER, Jeffery K, Bunnefeld N, et al (2020) Rare ground data confirm significant warming and drying in western equatorial Africa. PeerJ 8:e8732. https://doi.org/10.7717/peerj.8732
[19] Chakanyuka TL (2019) The Conservation of African Elephants under the CITES International Ivory Trade Ban. Kathmandu Sch L Rev (KSLR) Vol.7, Issue 2:p.71-83
[20] Chen G, Li K, Liu Y (2021) Applicability of Continuous, Stationary, and Discrete Wavelet Transforms in Engineering Signal Processing. Journal of Performance of Constructed Facilities 35:04021060. https://doi.org/10.1061/(ASCE)CF.1943-5509.0001641
[21] Chirwa PW, Adeyemi O (2020) Deforestation in Africa: Implications on Food and Nutritional Security. In: Leal Filho W, Azul AM, Brandli L, et al. (eds) Zero Hunger. Springer International Publishing, Cham, pp 197–211
[22] Cifuentes J, Marulanda G, Bello A, Reneses J (2020) Air Temperature Forecasting Using Machine Learning Techniques: A Review. Energies 13:4215. https://doi.org/10.3390/en13164215
[23] Daud SNSS, Sudirman R (2022) Wavelet Based Filters for Artifact Elimination in Electroencephalography Signal: A Review. Ann Biomed Eng 50:1271–1291. https://doi.org/10.1007/s10439-022-03053-5
[24] Dellink R, Hwang H, Lanzi E, Chateau J (2017) International trade consequences of climate change. OCDE, Paris
[25] Denis C, Varenne F (2022) Interprétabilité et explicabilité de phénomènes prédits par de l'apprentissage machine. Revue Ouverte d'Intelligence Artificielle 3:287–310. https://doi.org/10.5802/roia.32
[26] Dominguez D, Barriuso Pastor J, Pantoja-Díaz O, González-Rodríguez M (2023) Forecasting Worldwide Temperature from Amazon Rainforest Deforestation Using a Long-Short Term Memory Model. Sustainability 15:15152. https://doi.org/10.3390/su152015152
[27] Eltehiwy M, Abdul-Motaal AB (2023) A new Method for Computing and TestingThe significance of the Spearman Rank Correlation. Computational Journal of Mathematical and Statistical Sciences. https://doi.org/10.21608/cjmss.2023.229746.1015
[28] Ezugwu AE, Oyelade ON, Ikotun AM, et al (2023) Machine Learning Research Trends in Africa: A 30 Years Overview with Bibliometric Analysis Review. Arch Computat Methods Eng 30:4177–4207. https://doi.org/10.1007/s11831-023-09930-z
[29] Gad I, Hosahalli D (2022) A comparative study of prediction and classification models on NCDC weather data. International Journal of Computers and Applications 44:414–425. https://doi.org/10.1080/1206212X.2020.1766769
[30] Ghasemlounia R, Gharehbaghi A, Ahmadi F, Albaji M (2024) Developing a novel hybrid model based on deep neural networks and discrete wavelet transform algorithm for prediction of daily air temperature. Air Qual Atmos Health. https://doi.org/10.1007/s11869-024-01595-2

[31] Gong B, Langguth M, Ji Y, et al (2022) Temperature forecasting by deep learning methods. Geoscientific Model Development 15:8931–8956. https://doi.org/10.5194/gmd-15-8931-2022

[32] Gossler FE, Duarte MAQ, Villarreal F (2023) Design of Nearly-Orthogonal Symmetric Wavelet Filter Banks Based on the Wavelet Orthogonalization Process. Circuits Syst Signal Process 42:234–254. https://doi.org/10.1007/s00034-022-02111-6

[33] Grooten M, Almond REA (2018) Living Planet Report 2018: Summary. In: CABI Digital Library. WWF

[34] Guillaume S-C (2019) Apprendre Le Machine Learning en UNE semaine

[35] Guo T, Zhang T, Lim E, et al (2022) A Review of Wavelet Analysis and Its Applications: Challenges and Opportunities. IEEE Access 10:58869–58903. https://doi.org/10.1109/ACCESS.2022.3179517

[36] Guo Y, Zhao R, Zeng Y, et al (2018) Identifying scale-specific controls of soil organic matter distribution in mountain areas using anisotropy analysis and discrete wavelet transform. CATENA 160:1–9. https://doi.org/10.1016/j.catena.2017.08.016

[37] Haque E, Tabassum S, Hossain E (2021) A Comparative Analysis of Deep Neural Networks for Hourly Temperature Forecasting. IEEE Access 9:160646–160660. https://doi.org/10.1109/ACCESS.2021.3131533

[38] Hou J, Wang Y, Zhou J, Tian Q (2022) Prediction of hourly air temperature based on CNN–LSTM. Geomatics, Natural Hazards and Risk 13:1962–1986. https://doi.org/10.1080/19475705.2022.2102942

[39] Hu J, Wang X, Zhang Y, et al (2020) Time Series Prediction Method Based on Variant LSTM Recurrent Neural Network. Neural Process Lett 52:1485–1500. https://doi.org/10.1007/s11063-020-10319-3

[40] Inik O, Inik Ö, Öztaş T, Yuksel A (2022) Soil Temperature Prediction with Long Short Term Memory (LSTM). Türk Tarım ve Doğa Bilimleri Dergisi 9:779–785. https://doi.org/10.30910/turkjans.1101753

[41] Isabona J, Kehinde R (2019) MULTI-RESOLUTION BASED DISCRETE WAVELET TRANSFORM FOR ENHANCED SIGNAL COVERAGE PROCESSING AND PREDICTION ANALYSIS. FUDMA JOURNAL OF SCIENCES 3:6–15

[42] Jofipasi CA, Miftahuddin, Hizir (2018) Selection for the best ETS (error, trend, seasonal) model to forecast weather in the Aceh Besar District. IOP Conf Ser: Mater Sci Eng 352:012055. https://doi.org/10.1088/1757-899X/352/1/012055

[43] Kang H, Yang S, Huang J, Oh J (2020) Time Series Prediction of Wastewater Flow Rate by Bidirectional LSTM Deep Learning. Int J Control Autom Syst 18:3023–3030. https://doi.org/10.1007/s12555-019-0984-6

[44] Karaman K, Sainte Fare Garnot V, Wegner JD (2023) DEFORESTATION DETECTION IN THE AMAZON WITH SENTINEL-1 SAR IMAGE TIME SERIES. ISPRS Annals of the Photogrammetry, Remote Sensing and Spatial Information Sciences X-1-W1-2023:835–842. https://doi.org/10.5194/isprs-annals-X-1-W1-2023-835-2023

[45] Karevan Z, Suykens JAK (2020) Transductive LSTM for time-series prediction: An application to weather forecasting. Neural Networks 125:1–9. https://doi.org/10.1016/j.neunet.2019.12.030

[46] Kermabon M (2022) Vers une atténuation des conflits hommes-éléphants : Cas de l'aire protégée de Moukalaba-doudou au Gabon. Mémoire de recherche, Université Le Mans

[47] Kumar BBS, Satyanarayana PS (2022) A mixture of Noise Image Denoising using Sevenlets Wavelet Techniques. Trends in Sciences 19:4186–4186. https://doi.org/10.48048/tis.2022.4186

[48] Kwon H, Choi Y, Park H, et al (2022) Distillation Column Temperature Prediction Based on Machine-Learning Model Using Wavelet Transform. In: Yamashita Y, Kano M (eds) Computer Aided Chemical Engineering. Elsevier, pp 1651–1656

[49] Laguardia A, Gobush KS, Bourgeois S, et al (2021) Assessing the feasibility of density estimation methodologies for African forest elephant at large spatial scales. Global Ecology and Conservation 27:e01550. https://doi.org/10.1016/j.gecco.2021.e01550

[50] Lee H, Calvin K, Dasgupta D, et al (2023) IPCC, 2023: Climate Change 2023: Synthesis Report, Summary for Policymakers. Contribution of Working Groups I, II and III to the Sixth Assessment Report of the Intergovernmental Panel on Climate Change [Core Writing Team, H. Lee and J. Romero (eds.)]. IPCC, Geneva, Switzerland. https://doi.org/10.59327/IPCC/AR6-9789291691647.001. Accessed 19 Aug 2024

[51] Li C, Zhang Y, Ren X (2020) Modeling Hourly Soil Temperature Using Deep BiLSTM Neural Network. Algorithms 13:173. https://doi.org/10.3390/a13070173

[52] MAIDOU HM (2020) Gouvernance forestière et REDD+: le cas du projet de renforcement des capacités institutionnelles pour les forêts du bassin du Congo. La gouvernance forestière en Afrique centrale: Entre pratiques et politiques 261

[53] Mishra S, Bordin C, Taharaguchi K, Palu I (2020) Comparison of deep learning models for multivariate prediction of time series wind power generation and temperature. Energy Reports 6:273–286. https://doi.org/10.1016/j.egyr.2019.11.009

[54] Moazenzadeh R, Mohammadi B, Duan Z, Delghandi M (2022) Improving generalisation capability of artificial intelligence-based solar radiation estimator models using a bio-inspired optimisation algorithm and multi-model approach. Environ Sci Pollut Res 29:27719–27737. https://doi.org/10.1007/s11356-021-17852-1

[55] Moukodouma D-FB, Mbourou DRR, Nkoulembene CA, Denis C (2023) A temperatures variation favor human-elephant conflict in Gabon's Lékédi National Park. IJAERS 10:007–026. https://doi.org/10.22161/ijaers.108.2

[56] Ning G, Wang S, Yim SHL, et al (2018) Impact of low-pressure systems on winter heavy air pollution in the northwest Sichuan Basin, China. Atmospheric Chemistry and

Physics 18:13601–13615. https://doi.org/10.5194/acp-18-13601-2018

[57] Nounangnonhou TC, Fifatin F-XN (2016) Modélisation et simulation des tendances climatiques à l'horizon 2040 sur le bassin du fleuve Ouémé en République du Bénin

[58] Park I, Kim HS, Lee J, et al (2019) Temperature Prediction Using the Missing Data Refinement Model Based on a Long Short-Term Memory Neural Network. Atmosphere 10:718. https://doi.org/10.3390/atmos10110718

[59] Piccolroaz S, Calamita E, Majone B, et al (2016) Prediction of river water temperature: a comparison between a new family of hybrid models and statistical approaches. Hydrological Processes 30:3901–3917. https://doi.org/10.1002/hyp.10913

[60] Ponni alias Sathya S, Ramakrishnan S (2020) Non-redundant frame identification and keyframe selection in DWT-PCA domain for authentication of video. IET Image Processing 14:366–375. https://doi.org/10.1049/iet-ipr.2019.0341

[61] Qiu C (2023) A Method Using LSTM Networks to Impute Missing Temperatures in Temperature Datasets and to Predict Future Temperatures. Highlights in Science, Engineering and Technology 46:116–124. https://doi.org/10.54097/hset.v46i.7691

[62] Ren P, Liu Z, Zhou X, et al (2021) Strong controls of daily minimum temperature on the autumn photosynthetic phenology of subtropical vegetation in China. Forest Ecosystems 8:31. https://doi.org/10.1186/s40663-021-00309-9

[63] Roland ZKC, Ornella MN, Donald MI, et al (2016) Repartition Des Glossines Dans La Province De L'ogooue Ivindo Ancien Foyer De Trypanosomose Humaine Africaine. ESJ 12:281. https://doi.org/10.19044/esj.2016.v12n12p281

[64] Rus M, Fettich A, Kristan M, Ličer M (2023) HIDRA2: deep-learning ensemble sea level and storm tide forecasting in the presence of seiches – the case of the northern Adriatic. Geoscientific Model Development 16:271–288. https://doi.org/10.5194/gmd-16-271-2023

[65] Russell K (2024) Seasonal Variation Of Dew-Point Temperatures In The United States. https://temperatures.com/weather-and-climate/seasonal-variation-of-dew-point-temperatures-in-the-united-states/. Accessed 16 Sep 2024

[66] Shahbaztabar D, Alirezaee S, Ahmadi M, Heydari R (2018) A MC-CDMA system based on orthogonal filter banks of wavelet transforms and partial combining. AEU - International Journal of Electronics and Communications 94:128–138. https://doi.org/10.1016/j.aeue.2018.05.026

[67] Torre-Schaub M (2023) Agir sans attendre pour le climat: la clé d'un avenir vivable Commentaire de la synthèse du 6e rapport du GIEC approuvé et publié le 19 mars 2023. Énergie - Environnement - Infrastructures : actualité, pratiques et enjeux 3

[68] Toto E (2023) Agroecology alliance calls for more food at less cost to nature in Congo Basin. In: Mongabay Environmental News. https://news.mongabay.com/2023/08/agroecology-alliance-calls-for-more-food-at-less-cost-to-nature-in-congo-basin/. Accessed 17 Sep 2024

[69] Vanos J, Guzman-Echavarria G, Baldwin JW, et al (2023) A physiological approach for assessing human survivability and liveability to heat in a changing climate. Nat Commun 14:7653. https://doi.org/10.1038/s41467-023-43121-5

[70] Vapnik V (2013) The Nature of Statistical Learning Theory. Springer Science & Business Media

[71] Vecellio DJ, Wolf ST, Cottle RM, Kenney WL (2022) Evaluating the 35°C wet-bulb temperature adaptability threshold for young, healthy subjects (PSU HEAT Project). Journal of Applied Physiology 132:340–345. https://doi.org/10.1152/japplphysiol.00738.2021

[72] Vengatesan K, Mahajan SB, Sanjeevikumar P, et al (2018) Performance Analysis of Gene Expression Data Using Mann–Whitney U Test. In: Konkani A, Bera R, Paul S (eds) Advances in Systems, Control and Automation: ETAEERE-2016. Springer, Singapore, pp 701–709

[73] Vierra A, Razzaq A, Andreadis A (2023) Chapter 27 - Continuous variable analyses: t-test, Mann–Whitney U, Wilcoxon sign rank. In: Eltorai AEM, Bakal JA, Newell PC, Osband AJ (eds) Translational Surgery. Academic Press, pp 165–170

[74] Vikas Goyal, Ayay Yadav, Rahul Mukherjee (2022) Performance Evaluation of Machine Learning and Deep Learning Models for Temperature Prediction in Poultry Farming. https://ieeexplore.ieee.org/abstract/document/9791771. Accessed 16 Sep 2024

[75] Wall Emerson R (2023) Mann-Whitney U test and t-test. Journal of Visual Impairment & Blindness 117:99–100. https://doi.org/10.1177/0145482X221150592

[76] Wang X, Wang X, Wang L, et al (2021) A Distributed Fusion LSTM Model to Forecast Temperature and Relative Humidity in Smart Buildings. In: 2021 IEEE 16th Conference on Industrial Electronics and Applications (ICIEA). pp 1–6

[77] Xia K, Huang J, Wang H (2020) LSTM-CNN Architecture for Human Activity Recognition. IEEE Access 8:56855–56866. https://doi.org/10.1109/ACCESS.2020.2982225

[78] Yadav A, Jha CK, Sharan A (2020) Optimizing LSTM for time series prediction in Indian stock market. Procedia Computer Science 167:2091–2100. https://doi.org/10.1016/j.procs.2020.03.257

[79] Zameer A, Jaffar F, Shahid F, et al (2023) Short-term solar energy forecasting: Integrated computational intelligence of LSTMs and GRU. PLOS ONE 18:e0285410. https://doi.org/10.1371/journal.pone.0285410